

# Journal of Materials Chemistry C

Accepted Manuscript



This is an *Accepted Manuscript*, which has been through the Royal Society of Chemistry peer review process and has been accepted for publication.

*Accepted Manuscripts* are published online shortly after acceptance, before technical editing, formatting and proof reading. Using this free service, authors can make their results available to the community, in citable form, before we publish the edited article. We will replace this *Accepted Manuscript* with the edited and formatted *Advance Article* as soon as it is available.

You can find more information about *Accepted Manuscripts* in the [Information for Authors](#).

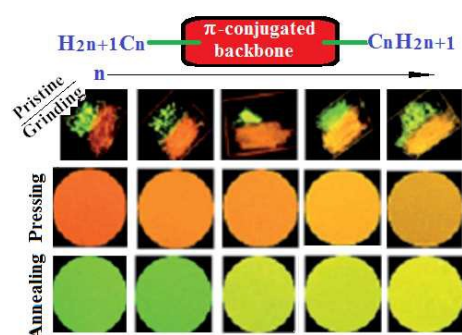
Please note that technical editing may introduce minor changes to the text and/or graphics, which may alter content. The journal's standard [Terms & Conditions](#) and the [Ethical guidelines](#) still apply. In no event shall the Royal Society of Chemistry be held responsible for any errors or omissions in this *Accepted Manuscript* or any consequences arising from the use of any information it contains.

# Alkyl length effects on solid-state fluorescence and mechanochromic behavior of small organic luminophores

Shanfeng Xue, Xu Qiu, Qikun Sun, Wenjun Yang\*

Key Laboratory of Rubber-Plastics of Ministry of Education/Shandong Provincial Key Laboratory of Rubber-Plastics; School of Polymer Science and Engineering, Qingdao University of Science & Technology, 53 Zhengzhou Road, Qingdao 266042, China. E-mail: [ywjph2004@qust.edu.cn](mailto:ywjph2004@qust.edu.cn)

This review focuses on alkyl length effects on solid-state fluorescence and mechanochromic behaviors, and the purpose is to arouse one's further attention to the alkyl-length effect in design, synthesis and structure–property investigation of organic optoelectronic materials.



# Alkyl length effects on solid-state fluorescence and mechanochromic behavior of small organic luminophores

Shanfeng Xue, Xu Qiu, Qikun Sun, and Wenjun Yang\*

Received (in XXX, XXX) Xth XXXXXXXXX 200X, Accepted Xth XXXXXXXXX 200X

First published on the web Xth XXXXXXXXX 200X

DOI: 10.1039/b000000x

The introduction of alkyl chains to the periphery of conjugated skeleton of organic chromophores is generally to improve the solubility. However, a number of investigations show that the length of alkyl chains could affect significantly the solid-state molecular packing modes, optical and electronic properties, thereby alkyl chains have played functional roles in tuning and altering the solid-state aggregation behavior and optoelectronic properties. While there have been a variety of reports on the impact of alkyl chains on organic field-effect transistor and photovoltaic performances, recently an increasing interest has paid to how the alkyl lengths affect the emission and stimuli responsive properties of organic fluorescent materials. This review focuses on alkyl length effects on solid-state fluorescence and mechanochromic behaviors, and the purpose is to arouse one's further attention to the alkyl-length effect in design, synthesis and structure-property investigation of organic optoelectronic materials.

## 1. Introduction

Conjugated organic molecules are promising materials for applications in optical, electronic, and optoelectronic fields. However, their large  $\pi$ -electron system and rigid skeleton make the solubility poor in common organic solvents and are not advantage for the processability and applications. In order to improve the solubility, a convenient and effective way is the introduction of alkyl chains to the periphery of conjugated skeleton. It has been known that the solution photo-physical properties of conjugated organic molecules are hardly affected by alkyl chain length, but there have been no much attention to the effects of alkyl chain lengths on the solid-state optical, electronic, and optoelectronic properties. A number of recent investigations have unambiguously again confirmed that alkyl length could influence intermolecular interactions, packing modes, and even molecular conformations in solid states, thus their solid-state optical and optoelectronic properties could be tuned and altered by subtle manipulation of peripheral alkyl groups.<sup>1-6</sup> From this perspective, alkyl chains have played functional roles in determining the solid-state aggregation behavior and optoelectronic properties of organic dyes. This is an interesting and valuable phenomenon since organic dyes with different length of alkyl chains make up the homologues with comparable molecular structure. Changing the alkyl length could not only manipulate subtly the peripheral groups to optimize intermolecular  $\pi$ - $\pi$  and aliphatic interactions and endow solid materials with unique and tunable optoelectronic properties, but also provide facile and valuable material systems for the investigation on structure-property correlation. Recently, increasing studies have shown that subtle changes of flexible side chains could have great impact on the device performance of organic field-effect transistors and solar cells,<sup>1-4</sup> which revealed the important role of flexible side chains in organic electronics and triggered the research of "side-chain engineering". In contrast, less attention has been paid to how the alkyl lengths affect solid-state fluorescence properties even if the tuning of alkyl length is simple. In this review, we describe recent studies on the effect of peripheral alkyl length on the solid-state fluorescence and mechano-

chromic behaviors and arouse one's further attention to the alkyl-length effect in the design, synthesis and structure-property investigation of organic optoelectronic materials.

## 2. The effect of alkyl length on aggregation behaviors and solid-state photo-physical properties

The extensively investigated luminophores exhibiting alkyl length-dependent fluorescence properties are those conjugated molecules with twisted backbone conformations, and these molecules usually show aggregation-induced emission (AIE) and mechanochromic luminescence phenomenon.<sup>7-10</sup> Dyes DVBC $n$  (Fig. 1) have twisted conjugated skeleton and exhibit weak solution fluorescence quantum yield ( $\Phi = 0.5$ –1.3%), but their crystals are of strong emission (data in Fig. 1).<sup>11</sup> The crystalline fluorescence efficiencies are related to alkyl length but change irregularly. The structure analysis of single crystals indicates that molecular conformation and packing mode are affected by alkyl length, and DVBC6 adopts the highly fluorescent J-aggregation mode.

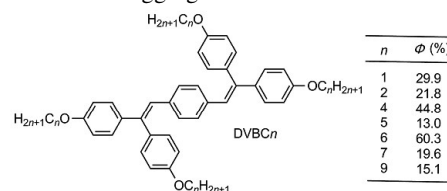


Fig. 1 Molecular structure and crystalline fluorescence efficiency of dyes DVBC $n$ . Reproduced from ref. 11 with permission. Copyright 2010 American Chemical Society.

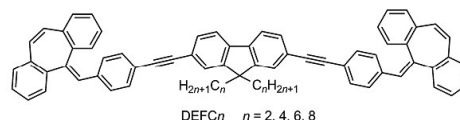


Fig. 2 Molecular structure of Dyes DEFC $n$ .

DEFC $n$  are capped with the twisted end moiety (Fig. 2) and are also AIE dyes. Their solid-state absorption and emission change with the length of alkyl chains, and the former is more obvious. When alkyl changes from ethyl, butyl, hexyl, to octyl, the peak absorption wavelengths of solid states are red-shifted by 59, 49, 40, and 33 nm relative to those of dilute solution, respectively.<sup>12</sup> This is ascribed to that long alkyl chain hinders intermolecular tight stacking.

1,4-Diaryl-butadienes (DAB) derivatives are also AIE dyes. Das et al. synthesized various DAB derivatives (Fig. 3) and elucidated the role of the number of alkoxy substituents and the length of alkyl chains in controlling the nature of the molecular packing and the fluorescence properties. In the di- and tri-alkoxy substituted derivatives (DBC $n$  and TBC $n$ ), the solid-state fluorescence properties was independent of the length of the alkyl chains.<sup>13</sup> But in the monoalkoxy substituted derivatives (MBC $n$ ), increasing the length of alkyl chains could result in a visual change in fluorescence from green to blue.<sup>14</sup> Based on the analysis of single crystals, this difference was attributed to fluorescence arising from aggregates with an edge-to-face alignment in the molecules possessing short alkyl chains (methyl and butyl) to monomer fluorescence in the long alkyl substituted derivatives. This study has provided a clear evidence for exciton splitting in the solid-state resulting in red-shifted emission for this class of materials.

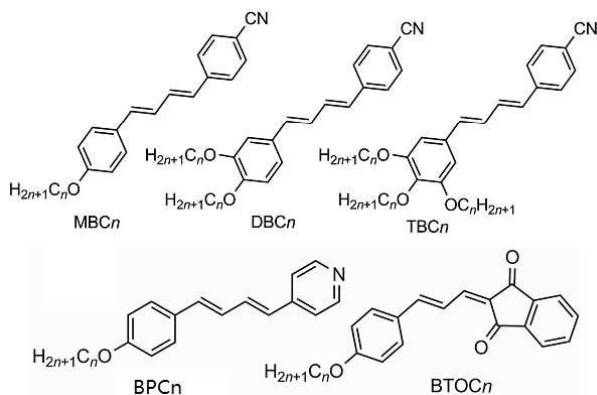


Fig. 3 Molecular structure of DAB derivatives.

Further, DAB derivatives with pyridine (BPC $n$ )<sup>15</sup> and 1,3-diketoindene (BTOC $n$ )<sup>16</sup> as acceptor were investigated (Fig. 3). A study of the melting behavior of BPC $n$  showed that, whereas BPC1 and BPC4 melted sharply from their crystalline to isotropic phase, BPC8 and BPC12 exhibited an intermediate phase in both the heating and cooling cycles. The intermediate phase showed the mosaic texture observed under polarized optical microscopy (POM) and was characteristic of a higher order smectic liquid crystalline phase. Powder X-ray diffraction (PXRD) studies however indicated it to be a plastic crystalline state. BPC4 showed heat-mode induced reversible polymorphism between two forms with significantly different fluorescence properties, making it a potentially useful material for thermal imaging applications. The difference in fluorescence behavior between films formed via slow cooling and rapid cooling could be attributed to a change in the molecular packing from a herringbone type arrangement in the slowly cooled films, to a brick-stone type arrangement in the

rapidly cooled films. The crystal packing of BTOC $n$  can be classified into three types. In type 1, observed for BTOC1, the molecules are virtually oriented one on top of the other to form a near perfect H-dimer. In type 2, observed for the dimers of BTOC4 and BTOC8, the molecules show substantial pitch displacement resulting in a head-to-tail arrangement of the neighboring molecules; however, since the pitch displacement is less than the length of the chromophore unit significant  $\pi$ -overlap still exists for these dimers. In type 3 packing, which is observed for BTOC12, the molecules are displaced substantially in the y direction resulting in virtually no  $\pi$ -overlap between the neighboring molecules. Thus BTOC $n$  derivatives provide a unique example wherein monomer, J-aggregate, and excimer emission could be observed from the same chromophore by varying its molecular packing either by varying the alkyl length (Fig. 4a) or by using external stimuli such as heat and light (Fig. 4b).

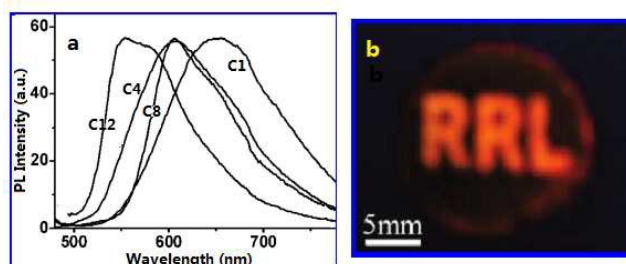


Fig. 4 Crystalline fluorescence spectra of BTOC $n$  (a) and image of BTOC8 thin film by irradiation with 445 nm light through a mask in which the unirradiated parts show red fluorescence on excitation with 365 nm light (b). Reproduced from ref. 16 with permission. Copyright 2009 American Chemical Society.

9,10-Bis(arylviny)anthracenes are a new class of AIE dyes with twisted structure. Tian et al found that the introduction of alkoxy chains and the extending of alkyl lengths could decreased the fluorescence efficiency (Fig. 5), which was ascribed to the suppression of molecular twisted degree and intermolecular interaction induced by alkoxy substitution based on structure analysis of single crystals.<sup>17</sup>

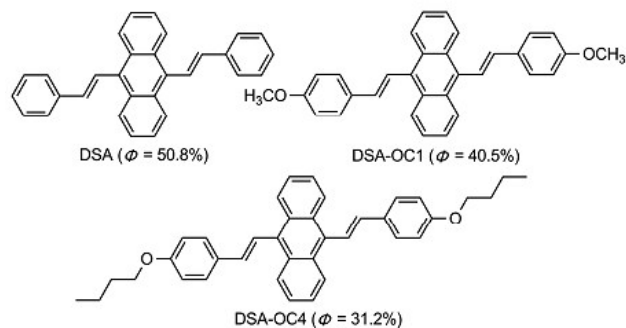
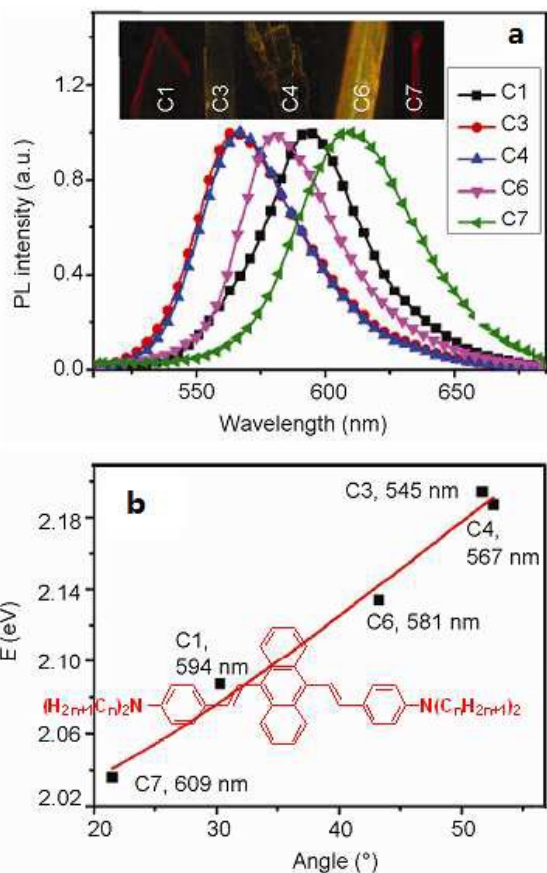


Fig. 5 Molecular structure and crystalline fluorescence efficiency ( $\Phi$ ) of 9,10-distyrylanthracene and its alkoxy derivatives.

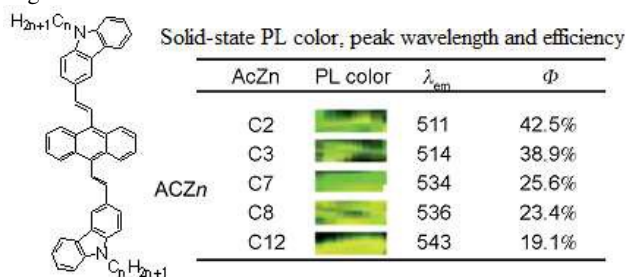
Changing the aryl end groups and alkyl lengths could synthesize various 9,10-bis(arylviny)anthracene homologues. Wang et al have synthesized 9,10-bis( $N,N$ -dialkylaminostyryl)-anthracenes (ASAC $n$ ) and found that crystalline ASAC1 and ASAC7 emit orange (594 nm) and red (609 nm) fluorescence with efficiencies of 59.4% and 52.0%, respectively, and

exhibit amplified spontaneous emission (ASE).<sup>18,19</sup> Other ASAC<sub>n</sub> were yellow emission and lower efficiency and no ASE. X-ray crystallographic analyses reveal that molecular packing modes (J- or H-aggregation) played an important role in determining the photo-physical properties, and the excitonic and dipolar couplings are both important for the optical properties of organic crystals.



**Fig. 6** Molecular structure (inset in Fig. 6b), crystalline fluorescence colors and spectra (a), and the relativity on peak emission energy with intermolecular slipping angle. Reproduced from ref. 19 with permission. Copyright 2014 Wiley-VCH.

A more regular alkyl length dependent homologue is 9,10-bis(*N*-alkylcarbazol-3-vinyl-2)anthracenes (ACZ<sub>n</sub>) studied by Wang et al.<sup>5</sup> It is observed that the crystalline emission wavelengths are gradually blue-shifted and the fluorescence efficiencies improved with the increase of alkyl lengths. This might be due to that longer alkyl chains are not advantageous to intermolecular tight stacking and suppressed the distortion degree of molecular conformations.



**Fig. 7** Molecular structure of ACZ<sub>n</sub> and their crystalline fluorescence color, emission peak wavelength (in nm), and fluorescence efficiency. Reproduced from ref. 5 with permission. Copyright 2012 The Royal Society of Chemistry.

However, it is noted that the peak emission wavelengths of pristine solids of 9,10-bis(*N*-alkylcarbazol-2-yl)vinyl-2]anthracenes (A2C<sub>n</sub>) are moderately blue-shifted from 548 to 530 nm with the increase of alkyl lengths.<sup>20</sup> This tendency is opposite to that observed in above ACZ<sub>n</sub> although the dependence of crystalline emission wavelength of A2C<sub>n</sub> on alkyl length is not strong as that of ACZ<sub>n</sub>. Of particular note is A2C<sub>n</sub> and ACZ<sub>n</sub>, they are aryl linking isomers.

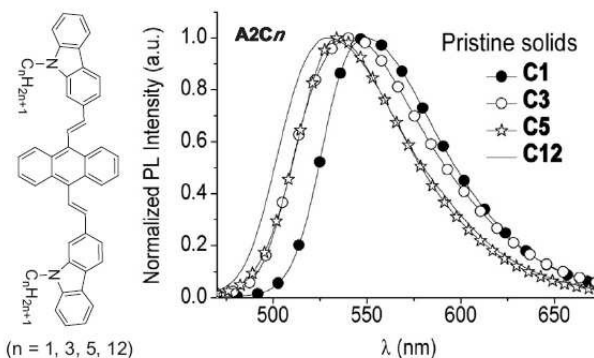
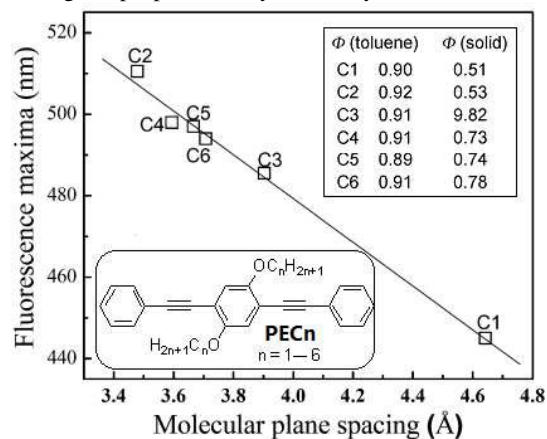


**Fig. 8** Molecular structure and crystalline emission spectra of A2C<sub>n</sub>. Reproduced from ref. 20 with permission. Copyright 2013 Elsevier B.V.

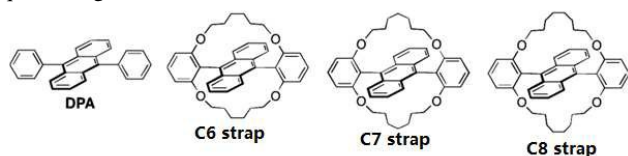
The reports on the effects of alkyl length on solid-state fluorescence of non-AIE active fluorophores are rare. One typical and systemic example is the influence of crystal packing on the solid state fluorescence behavior of alkoxy substituted 1,4-bis(phenylethynyl)benzene (PEC<sub>n</sub>, Fig. 9).<sup>21</sup> Although all molecules exhibit similar absorption and emission in dilute solutions, from methoxy to hexyloxy, the emission peaks are highly red shifted in the solid state. The red shift is maximum in ethoxy and minimum in methoxy, while other crystalline films exhibit intermediate values. In the crystal structures, the spacing varies from 3.48 to 4.65 Å between the molecular pairs forming the J-aggregates, with no systematic dependence on the chain length. The red shifted emission maximum is found to vary linearly with the spacing between the interacting molecules in the J-aggregate. Thus, the emission in the solid state is determined by the extent of dipolar coupling between the molecules, the alkyl chain length influencing the properties only indirectly.



55

**Fig. 9** Variation of the emission maximum with the spacing between the interacting molecules in crystals of PEC $n$  (excitation 360 nm). Molecular structure (bottom inset) and fluorescence efficiency in toluene or solid state (top inset). Reproduced from ref. 21 with permission. Copyright 2012 The Royal Society of Chemistry.

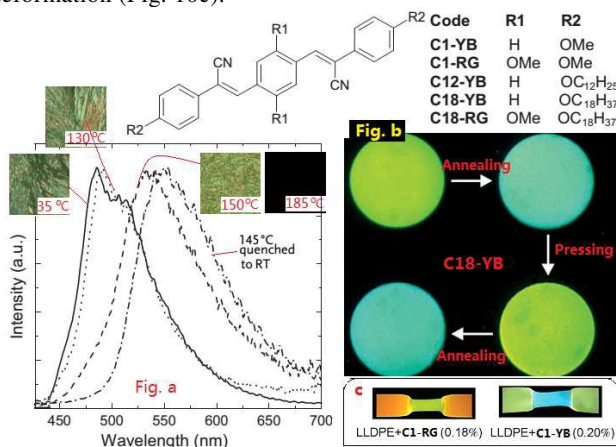
Kobayashi et al report the synthesis, photochemical and photophysical properties of double alkylene-strapped 9,10-diphenylanthracene derivatives ( $C_n$  straps) where the reactive central aromatic ring of the anthracene moiety is protected by the double alkylene straps (Fig. 10).<sup>22</sup> Thus,  $C_n$  straps were much more resistant to photochemical reactions than the parent 9,10-diphenylanthracene (DPA). Furthermore,  $C_7$  strap in benzene as well as in a cast film and the powder state showed the highest fluorescence quantum yields, wherein the  $C_7$  strap effectively serves to block fluorescence self-quenching.



**Fig. 10** Molecular structure of 9,10-diphenylanthracene and double alkyl-strapped derivatives ( $C_n$  straps).

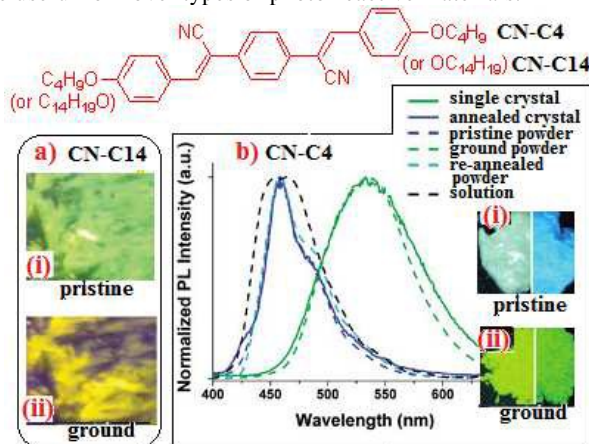
### 3. Alkyl length-dependent mechanochromic luminescence

Physically mechanochromic (MC) luminogens alter their emission by changing the molecular conformation or aggregate morphology and have attracted considerable attention due to their promising applications in mechanosensors, security papers, and optical storage.<sup>9,10,23</sup> The first report on alkyl length effect on MC behavior is Weder's  $\alpha$ -cyano-substituted oligo( $p$ -phenylene vinylene) derivatives ( $\alpha$ -cyano-OPVs, top in Fig. 11) in which the emission properties of  $C_{12}$ -YB and  $C_{18}$ -YB can be reversibly and repeatedly switched from monomer to excimer fluorescence upon quenching the compounds from a nematic state (Fig. 11a) or compression (Fig. 11b).<sup>24</sup> This is considered as the variation of electron density in the central ring and the length of peripheral aliphatic tails, which can balance  $\pi$ - $\pi$  and aliphatic interactions to produce desired properties. Although  $C_1$ -YB and  $C_n$ -RG themselves are non-MC active, the LLDPE films doped with  $C_1$ -YB or  $C_1$ -RG exhibit MC behavior upon deformation (Fig. 10c).<sup>25</sup>



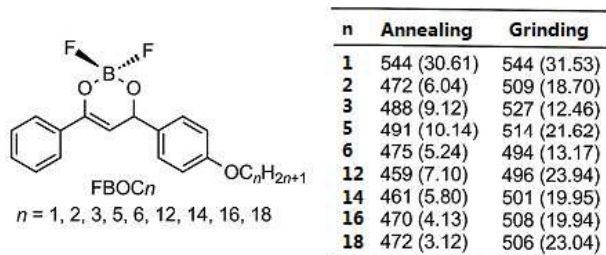
**Fig. 11** Molecular structure of  $\alpha$ -cyano-alkoxy-OPVs (top) and the cross-polarized optical micrographs and the corresponding emission spectra (a), the MC fluorescence images (b) of  $C_{18}$ -YB, and deformation-induced MC behavior of LLDPE film doped with  $C_1$ -RG or  $C_1$ -YB. Reproduced from ref. 24, 25 with permission. Copyright 2008 Wiley-VCH, 2003 American Chemical Society.

In contrast, pure isomer solids and PMMA film doped with short (CN-C4) and longer (CN-C14) alkoxy  $\beta$ -cyano-OPV are all MC active (Fig. 12).<sup>26,27</sup> Overall, there have been few reports on how the systematical change of alkyl length affects the solid-state fluorescence and stimuli response behavior. By the way, alkoxy-containing cyano-OPVs are light-unstable in both solution and liquid crystal phase, and this property could be useful for novel types of photo-reactive materials.<sup>27</sup>



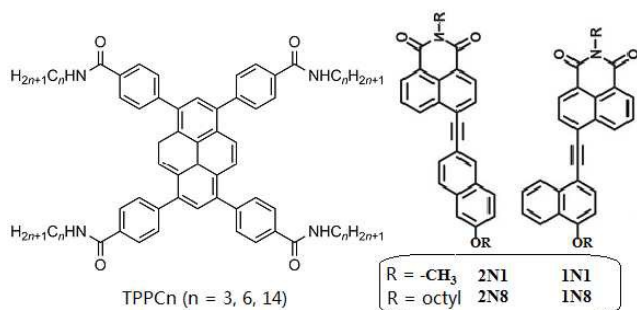
**Fig. 12** Molecular structure (top), fluorescence images of pristine (i) and ground (ii) powder of CN- $C_n$ , and emission spectra of CN-C4 under various states. Reproduced from ref. 26 with permission. Copyright 2010 American Chemical Society.

Chain length dependent emission was also observed for FBOC $n$  derivatives in both powders and slow evaporated films (Fig. 13).<sup>28,29</sup> All FBOC $n$  dyes but FBOC1 are MC luminescence active, and smearing has amorphized pristine crystals, red-shifted emission spectra, delayed fluorescence lifetime (data in parentheses), and activated excimer emission. The emission spectra under MC state as smeared powders on quartz surfaces were monitored at room temperature as a function of time. The recovery time generally increased with alkyl chain length, ranging from minutes ( $n = 3$ ) to days ( $n = 18$ ). Longer chain analogues ( $n = 6, 12, 14, 16, 18$ ) did not fully return to the original annealed emissive state even after months on quartz.



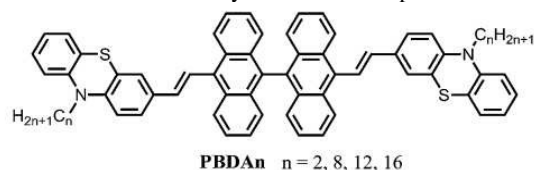
**Fig. 13** Molecular structure and peak emission wavelength (in nm) and fluorescence lifetime (in ns, data in parentheses) of annealed and ground FBOC $n$  solids. Reproduced from ref. 28 with permission. Copyright 2011 The Royal Society of Chemistry.

Fig. 14 depicts the molecular structure of alkyl-containing pyrene-amides (TPPC<sub>n</sub>) and naphthylethynyldiimides with different naphthyl linking positions (1N<sub>n</sub>, 2N<sub>n</sub>). C6 and C14 but not C3 of TPPC<sub>n</sub> exhibit obvious MC luminescence. It is thought that the proper long alkyl chain in TPPC<sub>n</sub> can change the twisting angles between the phenyl rings and pyrene unit and/or inhibit H-aggregation in the columnar assembled structures to lead to the change in luminescent color.<sup>30,31</sup> In the case of naphthyl-ethynyldiimides,<sup>32</sup> the solid-state colors of 2N1 and 1N8 change when the solution evaporation rates are relatively faster (yellow) and slower (yellow-orange or orange), while 2N8 and 1N1 only show one color (yellow-green), regardless of evaporation rates. Importantly, highly solvatochromic 1N8 solid displays thermochromic (orange to yellow), MC (orange to yellow) and vapochromic (yellow to orange) stimuli-responsive behavior. This is related to the packing change based on a 180° dyad rotation relative to the long axis of the molecule. Thus both the conjugated backbone and the alkyl length affect the solid-state optical properties and stimuli-responsive behavior.



**Fig. 14** Molecular structure of alkyl-containing pyrene-amides (TPPC<sub>n</sub>) and naphthylethynyldiimides.

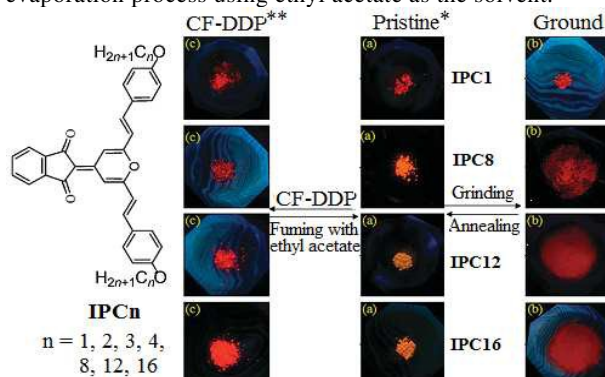
N-Alkylphenothiazine-9,9'-bianthryl derivatives (PBA<sub>n</sub>) are non-AIE active dyes, which is different from those 9,10-bis-arylviny molecules with monoanthracene as π-center.<sup>33-35</sup> PBA<sub>n</sub> emit strong fluorescence in both solution and solid state, and their solid-state fluorescence emissions and grinding-induced spectral shifts are related to alkyl length (Fig. 15).<sup>36</sup> Among them, PBA2 shows the smallest fluorescence and absorption spectrum shifts under mechanical force stimuli, and homologues with longer alkyl chains exhibit similar MC behavior and larger fluorescence contrasts after grinding. PXRD and differential scanning calorimetry (DSC) reveal that the transformation between crystalline and amorphous states upon various external stimuli is responsible for the MC behavior. Moreover, the fluorescence emission of ground solid PBA16 can recover at room temperature, which is ascribed to the low cold-crystallization temperature.



	$\lambda_{\text{abs}}$ (nm)		$\lambda_{\text{em}}$ (nm)		$\Delta\lambda_{\text{MC}}$ (nm)
	Pristine	Ground	Pristine	Ground	
<b>PBA2</b>	453	433	560	580	20
<b>PBA8</b>	418	433	513	568	55
<b>PBA12</b>	422	433	519	563	44
<b>PBA16</b>	422	441	517	559	42

**Fig. 15** Molecular structure (top) and absorption and emission wavelength under pristine and ground states (bottom) of 9,9'-bianthracene cored dyes PBA<sub>n</sub>. The ground-induced spectral shift  $\Delta\lambda_{\text{MC}} = \lambda_{\text{em}}(\text{ground}) - \lambda_{\text{em}}(\text{pristine})$ . Reproduced from ref. 36 with permission. Copyright 2012 The Royal Society of Chemistry.

Alkoxyalkyl-substituted indene-1,3-dione-pyrans (IPC<sub>n</sub>) are aggregation-induced emission (AIE) dyes. The pristine solids obtained by precipitating acetonitrile solution by methanol emit from red to yellow fluorescence with fluorescence efficiency of 2.5–7.1% when the increase of the length of the alkoxy chains.<sup>37</sup> When pristine solids are ground using a pestle in a mortar, all IPC8–16 but IPC1-4 change fluorescence color obviously from orange (IPC8) or yellow (IPC12, IPC16) to red, along with the further decrease of fluorescence efficiency. MC states could be restored to pristine states by both heat-annealing and ethyl acetate (EA)-fuming. Interestingly, evaporating the chloroform or THF solutions of pristine and ground IPC8–16 solids affords strong the red-emitting solids, similar to MC states. Moreover, thus obtained red solids could nearly be converted to the respective pristine solid states through EA-fuming or dissolution-evaporation process using ethyl acetate as the solvent.



Dyes	$\lambda_{\text{Pristine}}$	$\lambda_{\text{Ground}}$	$\lambda_{\text{CF-DDP}}$	$\Delta\lambda_{\text{MC}}$	$\Delta\lambda_{\text{CF-DDP}}$
<b>IPC1</b>	640	645	649	5	9
<b>IPC2</b>	627	628	638	1	11
<b>IPC3</b>	609	610	613	1	4
<b>IPC4</b>	602	609	612	7	10
<b>IPC8</b>	589	637	647	48	57
<b>IPC12</b>	567	611	633	44	66
<b>IPC16</b>	580	631	621	51	41

\*MeCN solution precipitated by MeOH;

\*\*Dissolved in CH<sub>2</sub>Cl<sub>2</sub> or THF and then evaporated.

**Fig. 16** Molecular structure and solid-state fluorescence images and the corresponding spectroscopic data of indene-1,3-dione-pyrans (IPC<sub>n</sub>) under various external stimuli. Reproduced from ref. 37 with permission. Copyright 2015 The Royal Society of Chemistry.

Strongly twisted 9,10-bis(arylvinyl)anthracenes are AIE and MC luminogens, and introducing alkyl chains to different aryl groups could afford various homologues. Recent studies show that MC behavior of various 9,10-bis(arylvinyl)anthracenes exhibit strong dependence on the peripheral alkyl length. The first series is 9,10-bis(*p*-alkoxystyryl)anthracene derivatives (DSA-*p*OC<sub>n</sub>).<sup>38,39</sup> The results show that longer alkoxy DSA-*p*OC<sub>n</sub> ( $n \geq 10$ ) exhibit remarkable grinding-induced spectral shifts ( $\Delta\lambda_{\text{MC}} = 46\text{--}53$  nm) that are significantly larger than those with shorter alkyl chains ( $n \leq 9$ ,  $\Delta\lambda_{\text{MC}} = 14\text{--}20$  nm) (positive effect). PXRD indicates that ground solids are still crystalline but the packing modes have been changed. DSC curves indicate that almost all of the DSA-*p*OC<sub>n</sub> exhibit two

exothermic peaks and the peaks in lower-temperature zone (P1) are influenced by grinding. P1 peak has been ascribed to phase transition from solid crystalline to liquid crystal by Chi et al based on the thermotropic liquid crystalline texture of DSA-*pOC11*.<sup>38,40</sup> However, the existence of P1 transition and its change upon grinding is not related to MC behavior or alkoxy length dependence since DSA-*pOC1* without P1 transition still shows moderate MC behavior. Moreover, some DSA-*pOCn* with  $n \leq 9$  exhibit very flat and broad P1 peak upon grinding but still show small  $\Delta\lambda_{MC}$  value.<sup>39</sup> Single crystal analyses show that the crystal density and supramolecular interactions of the DSA-*pOCn* with  $n \geq 10$  are somewhat lower than that of other DSA-*pOCn* with  $n \leq 9$ , but the dihedral angles between the phenyl rings and anthryl ring are contrary. This could be regarded as a probable reason why DSA-*pOCn* with  $n \geq 10$  exhibit blue-shifted emissions and remarkable MC behavior since the relatively loose molecular packing, weak intermolecular interactions, and more twisted conformation could decrease the lattice energies and  $\pi$ -conjugation degree and enhance inner stress to render such crystals easily destructible upon external force stimuli. It is noted that, for most MC materials, pressing the samples exhibits the same effectiveness as grinding for the changes in fluorescence colors and emission wavelengths, as well as  $\Delta\lambda_{MC}$ .

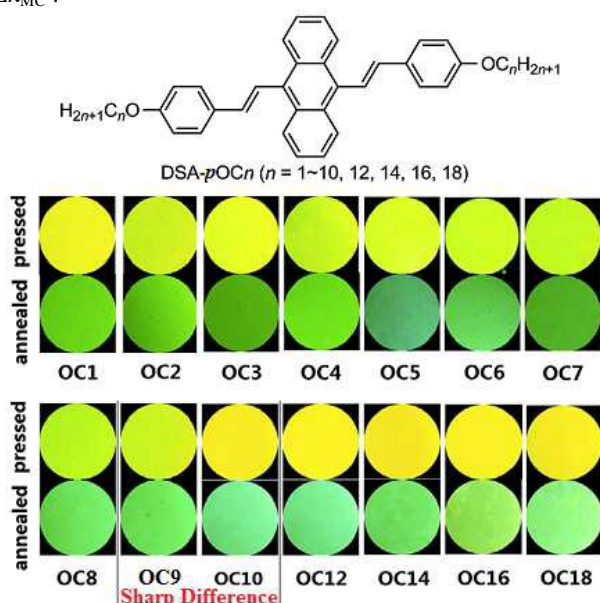


**Fig. 17** Molecular structure of DSA-*OCn* (top), and the fluorescence images of DSA-*OCn*-KBr mixture upon pressing with IR pellet press (pressed) and heat-annealing (annealed) illuminated by a UV lamp of 365 nm (same for below images). Reproduced from ref. 39 with permission. Copyright 2013 Elsevier B.V.

However, changing the linking positions of alkoxy chains at styryl ring can significantly alter the AIE and MC activities of 9,10-bis(alkoxystyryl)anthracenes.<sup>41</sup> In THF solutions (Fig. 18), the  $\Phi$  values are in the order  $\Phi_{pOCn} < \Phi_{oOCn} < \Phi_{mOCn}$ , which can be ascribed to the increasing electron-donating ability of the alkoxy moiety to the conjugated backbone from meta-, ortho- to para-linkages (electronic effect). On the other hand, the fluorescence emissions become weaker, broader and more red-shifted from meta, ortho to para-isomers, implying the existence of increasing amplitude relaxation in the excited state. That is, the non-symmetric introduction of a substituent relative to the intramolecular torsion motion (ITM) axle could

hamper ITM and reduce the nonradiative decay (steric effect). In aqueous media, the  $\Phi$  values of *pOCn* (the strongest AIE effect), *mOCn* (the weakest) and *oOCn* (moderate) are 47–67, 41–46 and 21–25%, respectively (numbers below the images in Fig. 18), respectively.

Fig. 19 shows that all *OCn* solids exhibit fluorescence color and spectral shift changes under external stimuli, but they are obviously both alkoxy position- and length-dependent. When changing the linking positions of alkoxy chains at styryl ring, the resulting new isomers (*oOCn* and *mOCn*) exhibit different alkoxy-related MC behaviour from *pOCn* (i.e., DSA-*pOCn*, Fig. 17). Instead, short alkoxy *OCn* (such as *oOC3* and *mOC3*) become highly MC active, and the  $\Delta\lambda_{MC}$  values of *oOC3* (55 nm) and *mOC3* (45 nm) are even higher than those of *pOC16* and *mOC16* respectively (data shown in Fig. 19). New long alkoxy *OCn* (such as *oOC16* and *mOC16*) show the decreased  $\Delta\lambda_{MC}$  compared to *pOC16*. Crystal structure analyses evidence that both alkoxy length and linking position influence molecular backbone conformations and the intermolecular interactions,<sup>41</sup> suggesting that changing the nature and linking position of substituents at aryl rings of 9,10-bis(arylvinyl)anthracenes could tune and alter the solid-state photo-physical properties and alkyl length dependence.

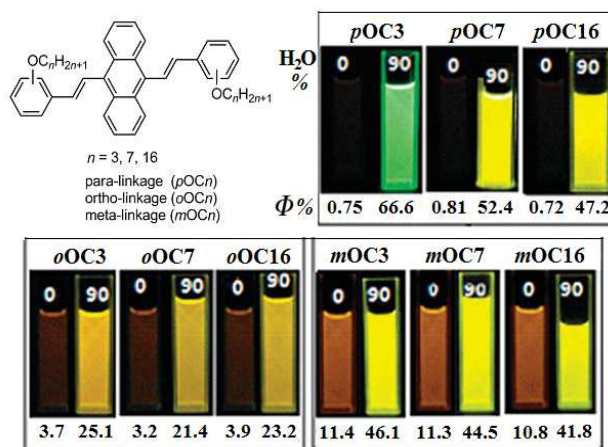
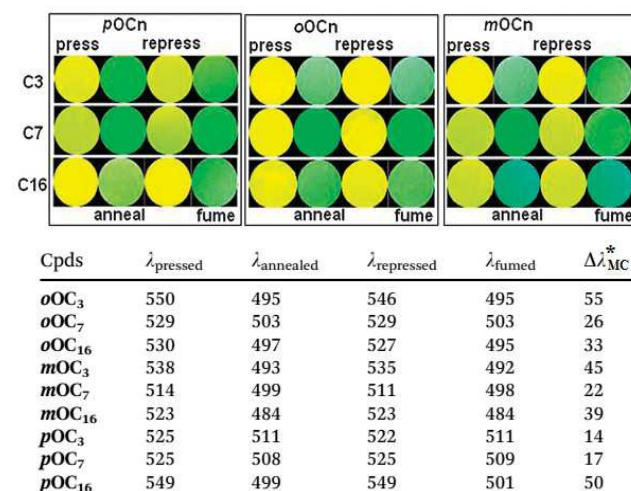


**Fig. 18** Molecular structure of *OCn* with different linking positions and the fluorescence images of *OCn* in THF (H<sub>2</sub>O 0%) and THF/water (1/9, H<sub>2</sub>O 90%). The numbers below the images are the corresponding relative fluorescence quantum yield. Reproduced from ref. 41 with permission. Copyright 2013 The Royal Society of Chemistry.



\* Pressing-induced spectral shift,  $\Delta\lambda_{MC} = \lambda_{\text{pressed}} - \lambda_{\text{annealed}}$ .

**Fig. 19** Fluorescence images and emission data of different OC $n$ -KBr mixtures under various external stimuli states. Reproduced from ref. 41 with permission. Copyright 2013 The Royal Society of Chemistry.

Recently, Wang and Bu et al. have designed and synthesized a series of 9,10-bis[(*N*-alkylcarbazol-3-yl)vinyl]anthracenes (AC $Zn$ )<sup>5</sup> and 9,10-bis[(*N*-alkylcarbazol-2-yl)vinyl-2]anthracenes (A2C $n$ )<sup>20</sup> to systematically investigate the effect of alkyl chain length on the solid-state fluorescence properties. AC $Zn$  and A2C $n$  are isomers. AC $Zn$  solids exhibit not only reversibly pronounced red-shift MC luminescence, but also strong and regular alkyl length dependent fluorescence properties (Fig. 20). Since emission spectra of pristine and ground AC $Zn$  solids are respectively red-shifted and blue-shifted with the increase of *N*-alkyl chain length, resulting in the shorter the *N*-alkyl chains, the more remarkable the MC behaviour (negative effect). Grinding- or pressing-induced spectra shift ( $\Delta\lambda_{MC}$ ) of ACZ2 solid is up to 88 nm and is among the highest value under simple mechanical force reported to date. AC $Zn$  is also a typical crystallization-enhanced emission dyes, and the solid-state fluorescence efficiencies are decreased upon grinding or with the increase of *N*-alkyl chain length.<sup>5</sup> PXRD and DSC reveal that these optical properties of AC $Zn$  are ascribed to the transformation between crystalline and amorphous states upon external stimuli.

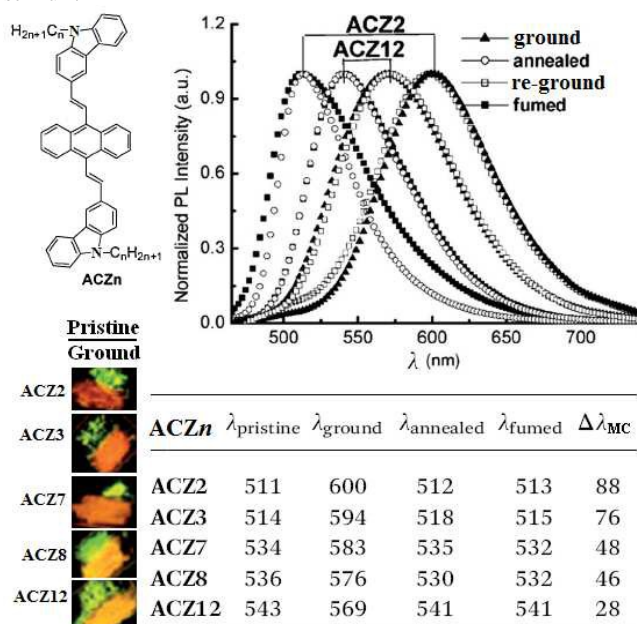
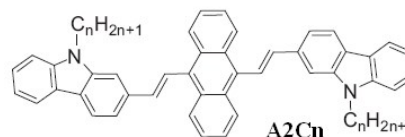


**Fig. 20** Molecular structure of AC $Zn$ , emission spectra, fluorescence images and emission data of pure AC $Zn$  solids under pristine and various external stimuli states. Reproduced from ref. 5 with permission. Copyright 2012 The Royal Society of Chemistry.

Unlike its isomer 9,10-bis[(*N*-alkylcarbazol-3-yl)vinyl-2]-anthracenes (AC $Zn$ ), alkyl lengths do not significantly affect the solid-state fluorescence emission and MC behavior of 9,10-bis[(*N*-alkylcarbazol-2-yl)vinyl-2]anthracenes (A2C $n$ )<sup>20</sup> (Fig. 21). These findings imply that the nature of end-arylene has played an important role in determining the effect of alkyl lengths on solid-state optical properties of organic luminogens, at least for 9,10-bis(arylvinyl)anthracene derivatives, and the subtle manipulation of end groups and alkyl chains could endow 9,10-bis(arylvinyl)anthracenes with unique and diverse solid-state optical properties. At present, the real origin for this dichotomous alkyl chain length-dependent fluorescence

and MC behaviour is not clear at present, underlining the complexity of the structure–property relationship.



Peak emission wavelengths ( $\lambda$ , in nm) of A2C $n$  samples upon external stimuli.

A2C $n$	$\lambda_{pristine}$	$\lambda_{pressed}$	$\lambda_{annealed}$	$\lambda_{repressed}$	$\lambda_{fumed}$	$\Delta\lambda_{MC}$
A2C1	548	572	536	572	541	36
A2C3	543	579	537	577	540	42
A2C5	535	578	533	575	533	45
A2C12	530	571	527	572	530	44

**Fig. 21** Molecular structure of A2C $n$ , fluorescence emission data under pristine and various external stimuli states. Reproduced from ref. 20 with permission. Copyright 2013 Elsevier B.V.

9,10-Bis(arylvinyl)anthracene derivatives have become one mainstay of MC materials reported to date. To further evaluate the effect of alkyl length on solid-state fluorescence and MC luminescence, 9,10-bis(*N*-alkylphenothiazin-3-ylvinyl-2)anthracenes (PT-C $n$ )<sup>42</sup> and 9,10-bis(*N*-alkylindole-3-ylvinyl-2)anthracenes (IAC $n$ )<sup>43</sup> with different chain length are prepared.

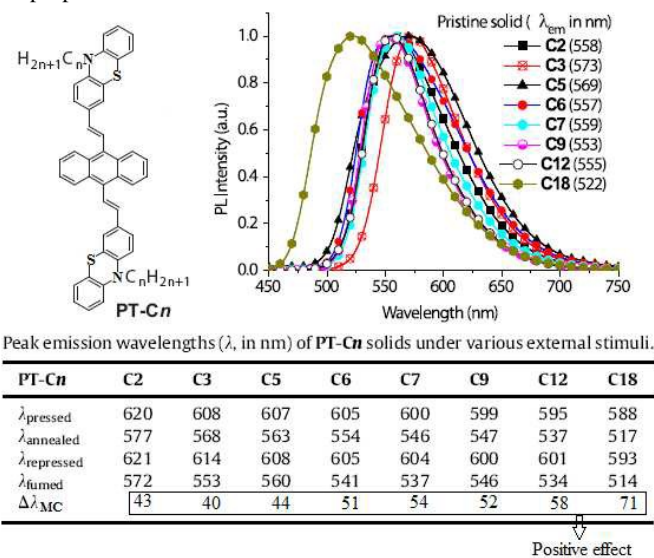
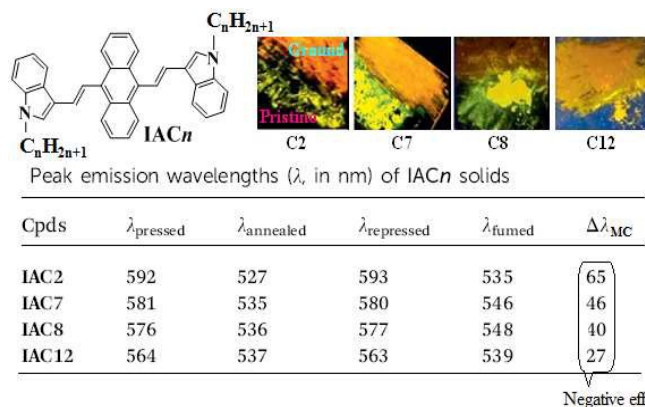


**Fig. 22** Molecular structure of PT-C $n$ , fluorescence spectra of pure solids, and emission data under various external stimuli states. Reproduced from ref. 42 with permission. Copyright 2014 Elsevier B.V.



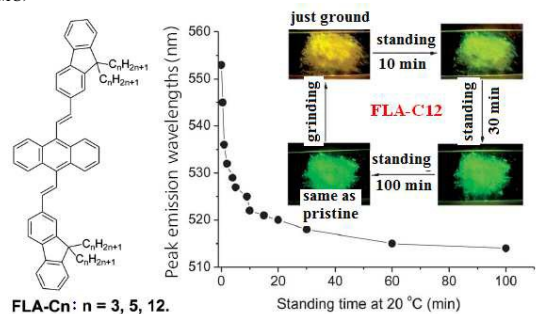
Negative effect

**Fig. 23** Molecular structure of IAC $n$ , fluorescence images of pure pristine and ground solids, and emission data under various external stimuli states. Reproduced from ref. 43 with permission. Copyright 2015 The Royal Society of Chemistry.

Fig.22 indicates that the emission spectra of pristine PT- $C_n$  solids are related to the alkyl length but irregular. However, the fluorescence colors and peak-wavelengths of both pressed and annealed (fumed) PT- $C_n$  solids are gradually blue-shifted; moreover, the blue-shift amplitude of annealed states is more remarkable with the increase of alkyl length (data in the lower part of Fig.22). The general trend of  $\Delta\lambda_{MC}$  values is the increase with the alkyl chain length, i.e., MC behavior of PT- $C_n$  is a positive alkyl-length effect. In contrast to PT- $C_n$ , it is found that the shorter the  $N$ -alkyl chain of IAC $n$ , the more remarkable the PFC behavior (Fig. 23), which is the same as those observed in ACZ $n$  and DSA- $pOC_n$  (Fig. 17 and Fig. 20), i.e., a negative alkyl-length effect.

#### 4. Regularly tuning the heat recovering temperature of MC luminescence materials by alkyl length effect

Organic MC luminogens exhibiting tunable heat recovering behavior should be promising materials suitable for various potential applications. It has been shown that, in most, but not all, MC materials, the reversible change in their fluorescence color and emission wavelength could be ascribed to the phase transition between crystalline and amorphous states. Therefore, controlling the cold-crystallization temperature of amorphous states ( $T_{cc}$ ) should be an effective way for tuning the heat recovering behavior. However, the chromophores substituted by mono- and bis-alkyl chains do not show regular  $T_m$  and  $T_{cc}$  changes with the length of alkyl chains. In 2013, Bu et al. reported the fluorescence emission and thermal transition behaviors of solid-state 9,10-bis[(9,9-dialkylfluorene-2-yl)-vinyl]anthracenes (FLA- $C_n$ ) under pristine and ground states (Fig. 24).<sup>44</sup> It is observed that, with the increase of the length of alkyl chains, the blue-shift amplitude of emission peak-wavelength of pristine solids is larger than that of ground solids, resulting in a gradually increasing MC spectral shift ( $\Delta\lambda_{MC}$ ).



Peak emission wavelengths (nm) and thermal transition temperature							
Cpd	$\lambda_{pristine}$	$\lambda_{ground}$	$\lambda_{annealed}$	$\lambda_{fumed}$	$\Delta\lambda_{MC}^a$	$T_m^b/^\circ C$	$T_{cc}^c/^\circ C$
FLA-C3	558	574	556	556	18	281	145
FLA-C5	530	554	528	532	26	180	132
FLA-C12	514	554	514	515	40	65	$\leq RT^d$

<sup>a</sup>  $\Delta\lambda_{MC} = \lambda_{ground} - \lambda_{annealed}$ . <sup>b</sup> Isotropic melt transition temperature. <sup>c</sup> Cold-crystallization temperature of ground solids. <sup>d</sup> Estimated.

**Fig. 24** Molecular structure of FLA- $C_n$ , fluorescence restoration process of ground FLA-C12 solid at RT, and fluorescence emission and thermal transition data of PLA- $C_n$  solids under various states. Reproduced from ref. 44 with permission. Copyright 2013 The Royal Society of Chemistry.

PXRD and DSC analyses of pristine and ground FLA- $C_n$  solids reveal the happen of phase transition between crystalline and amorphous states upon external stimuli. From DSC experiment, the gradual decrease of both isotropic melting temperature ( $T_m$ ) and amorphous-state  $T_{cc}$  are observed with the increase of alkyl length. An intriguing MC behavior is the spontaneous recovery of fluorescence emission and color of ground FLA-C12 solid at room temperature (RT). Amorphized FLA-C3 and FLA-C5 solids have high  $T_{cc}$  values, rendering their MC state stable at RT. Since  $T_{cc}$  value, to a given compound, is greatly lower than its  $T_m$ , the  $T_{cc}$  of ground FLA-C12 solid should be at or below RT. This is why the ground FLA-C12 solid exhibits the spontaneously recovering fluorescence properties upon standing at RT (Fig. 24).

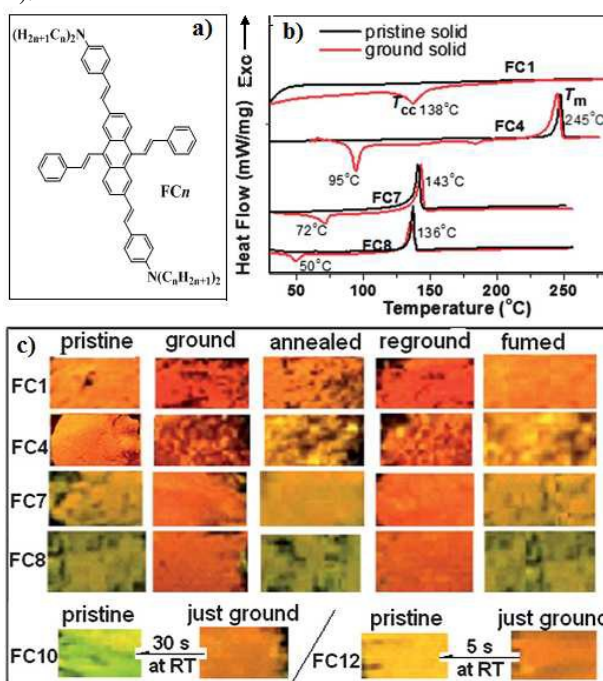


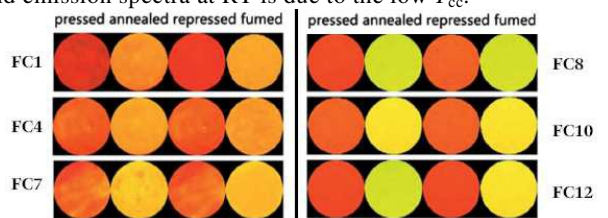
**Fig. 25** Molecular structure of cruciform  $FC_n$ , DSC curves and fluorescence images of pure  $FC_n$  solids under various states. Reproduced from ref. 45 with permission. Copyright 2013 The Royal Society of Chemistry.

Recently, Zheng et al. have synthesized cruciform 2,6,9,10-tetrastyryl anthracenes containing four alkyl chains ( $FC_n$ , Fig 25a).<sup>45</sup> This dye could be regarded as the cross-integrate of 2,6-bis-(dialkylaminostyryl)anthracene (2,6-branch) and 9,10-di-styrylanthracene (9,10-branch). Although the two branches hardly show MC behavior, the cruciform  $FC_n$  do exhibit MC luminescence (Fig. 25c). When simply ground the pure  $FC_n$  solids on the glass plate using a metal spatula, the fluorescence colors of the ground  $FC_1$ – $FC_8$  solids are stable and remain unchanged over 24 hours at room temperature, but ground  $FC_{10}$  and  $FC_{12}$  solids can spontaneously change back to original colors within seconds at room temperature (Fig. 25c). Considering that the difference among these cruciforms is only the  $N$ -alkyl length, it is concluded that the alkyl chains play a crucial role in determining the solid-state optical properties and the heat-recovery behavior of the ground states.

Meanwhile, the pressing experiment of the  $FC_n$ -KBr mixture ( $FC_n$  solid (5–7 mg) mixed with KBr (50 mg)) with

an IR pellet press are conducted at room temperature. Overall, the pressing gives the same effectiveness as the grinding, and the fluorescence colors can reversibly be changed by heat-annealing, solvent-fuming, and repressing (Fig. 26a).  
 Interestingly, the fluorescence colors of the pressed FC10 and FC12 samples can remain almost unchanged over 5 min at room temperature, implying that KBr matrix could decrease molecular motion of the dispersed fluorophores and delay the recovery process, and thus allowing the spectral measurement.  
 It is observed that the longer the alkyl chain length, the larger the  $\Delta\lambda_{MC}$  values (table in Fig. 26), i.e., FC $n$  is also a MC homologue with positive alkyl-length effect.

To understand the PFC mechanism and the effect of  $N$ -alkyl chains on the thermal-recovering behaviour of cruciform FC $n$  solids, PXRD and DSC experiments on pristine and ground FC1–FC8 solids were conducted and evidence the phase transformation between crystalline and amorphous states upon external stimuli. DSC experiments indicate no thermal transitions for the pristine solids before  $T_m$ ; however, each of ground solids shows the respective cold-crystallization transition (Fig. 25b). Increasing the  $N$ -alkyl length of FC $n$  can regularly not only enlarge the  $\Delta\lambda_{MC}$  but also decrease the  $T_{cc}$  of ground states (table in Fig. 26) to render the MC materials with tunable heat-recovery temperature. Ground FC10 and FC12 solids can spontaneously self-recover fluorescence color and emission spectra at RT is due to the low  $T_{cc}$ .



Peak emission wavelengths (nm) and thermal transition data of FC $n$  solids

FC $n$	$\lambda_{\text{pristine}}$	$\lambda_{\text{pressed}}$	$\lambda_{\text{annealed}}$	$\lambda_{\text{re-pressed}}$	$\lambda_{\text{fumed}}$	$\Delta\lambda_{MC}$	$T_m$ /°C	$T_{cc}$ /°C
FC1	591	616	593	615	593	23	>300	138
FC4	597	613	588	613	588	25	245	95
FC7	563	595	565	593	563	30	143	72
FC8	541	598	544	597	547	54	136	50
FC10	538	597	552	597	554	45	nd <sup>a</sup>	≤RT
FC12	551	596	547	597	555	49	nd	<RT

<sup>a</sup> Not determined. <sup>b</sup> Estimated.

**Fig. 26** Fluorescence images of FC $n$ -KBr mixtures upon external stimuli and the fluorescence emission and thermal transition data under the corresponding solid states. Reproduced from ref. 45 with permission. Copyright 2013 The Royal Society of Chemistry.

## 5. Conclusion and outlook

In summary, this article has reviewed recent investigations on the effect of alkyl length on solid-state fluorescence emission and mechanochromic behaviors based on small organic dyes. Most conjugated organic molecules synthesized artificially consist of  $\pi$ -conjugated backbones and peripheral flexible side chains. Flexible side chains are insulating and non-fluorescent in nature and do not directly contribute to the charge transport and fluorescence emission properties. Consequently most research efforts have focused on the  $\pi$ -conjugated backbones, and the flexible side chains are generally regarded as the solubilizing groups and have not been fully exploited even though numerous side chain substituents have been tested over

the years. The present examples indicate that, apart from the conjugated backbones, the alkyl chain length, linking position and density all have important impact on the solid-state molecular packing and microstructure, as a result, the solid-state optical, optoelectronic properties, and stimuli-responsive behaviors could be tuned or altered. Therefore, much attention should be paid to the alkyl-length effect in design, synthesis and structure–property investigation of organic optoelectronic materials even if their influence on aggregation microstructure and fluorescence behaviors is complex and often irregular. The “side-chain engineering” can become an important part of molecular engineering since alkyl chains are the most commonly used side chains in conjugated organic molecules, and tuning the alkyl chain length is the simplest strategy. In this context, small  $\pi$ -conjugated molecules with well-defined structures are more suitable for the study of the influence of alkyl chain length on the optical and optoelectronic properties.

In spite of these interesting materials and phenomena, further systematic investigation on alkyl length-dependent molecular packing and fluorescence properties is still a challenging topic because the introduction of longer alkyl chain usually makes single-crystal growth more difficult and limits in-depth understanding of molecular packings and solid-state properties. It is also difficult to estimate proper alkyl chain length and density for obtaining a better balance among good solubility, unique intermolecular stacking, and desired novel properties.

## Acknowledgment.

We thank the NSFC of P. R. China (No. 51073083, 51173092, 51303091, and 51473084), NSF of Shandong Province (No. 2014ZRB01296), China Postdoctoral Science Fund (2015M582061, 2014M 560537), Open Project of State Key Laboratory of Supramolecular Structure and Materials of Jilin University (SKLSSM-2016xx), and Specialized Research Fund for the Doctoral Program of Higher Education (No. 201333719120005).

## Notes and references

- Key Laboratory of Rubber–Plastics of Ministry of Education/Shandong Provincial Key Laboratory of Rubber-plastics, School of Polymer Science and Engineering, Qingdao University of Science & Technology, 53 Zhengzhou Road, Qingdao 266042, China.  
 E-mail: ywjph2004@qust.edu.cn
- J. Mei, and Z. Bo, *Chem. Mater.*, 2014, **26**, 604–615.
  - F. Zhang, Y. Hu, T. Schuettfort, C. Di, X. Gao, C. R. McNeill, L. Thomsen, S. C. B. Mannsfeld, W. Yuan, H. Sirringhaus, and D. Zhu, *J. Am. Chem. Soc.*, 2013, **135**, 2338–2345.
  - X. Y. Wang, F. D. Zhuang, X. Zhou, D. C. Yang, J. Y. Wang, and J. Pei, *J. Mater. Chem. C*, 2014, **2**, 8152–8161.
  - J. Y. Back, T. K. An, Y. R. Cheon, H. Cha, J. Jang, Y. Kim, Y. Baek, D. S. Chung, S. K. Kwon, C. E. Park, and Y. H. Kim, *ACS Appl. Mater. Interfaces*, 2015, **7**, 351–358.
  - Y. Wang, W. Liu, L. Bu, J. Li, M. Zheng, D. Zhang, M. Sun, Y. Tao, S. Xue and W. Yang, *J. Mater. Chem. C*, 2013, **1**, 856–862.
  - W. Liu, Y. Wang, L. Bu, J. Li, M. Sun, D. Zhang, M. Zheng, C. Yang, S. Xue, W. Yang, *J. Lumin.*, 2013, **143**, 50–55.
  - Y. N. Hong, J. W. Y. Lam, and B. Z. Tang, *Chem. Soc. Rev.*, 2011, **40**, 5361–5388.
  - Q. Y. Wu, Q. Peng, T. Zhang, and Z. G. Shuai, *Scientia Sinica Chimica*, 2013, **43**, 1078–1089.
  - Z. Chi, X. Zhang, B. Xu, X. Zhou, C. Ma, Y. Zhang, S. Liu, and J. Xu, *Chem. Soc. Rev.*, 2012, **41**, 3878–3896.
  - Y. Q. Dong, J. W. Y. Lam, and B. Z. Tang, *J. Phys. Chem. Lett.*, 2015, **6**, 3429–3436.

- 11 P. An, Z. F. Shi, W. Dou, X. P. Cao, and H. L. Zhang, *Org. Lett.*, 2010, **12**, 4364–4367.
- 12 Z. X. Wang, H. X. Shao, J. C. Ye, L. Tang, P. Lu, *J. Phys. Chem. B*, 2005, **109**, 19627–19633.
- 13 R. Davis, N. S. S. Kumar, S. Abraham, C. H. Suresh, N. P. Rath, N. Tamaoki, and S. Das, *J. Phys. Chem. C*, 2008, **112**, 2137–2146.
- 14 R. Davis, N. P. Rath, and S. Das, *Chem. Commun.*, 2004, 74–75.
- 15 N. S. S. Kumar, S. Varghese, N. P. Rath, and S. Das, *J. Phys. Chem. C*, 2008, **112**, 8429–8437.
- 16 N. S. S. Kumar, S. Varghese, C. H. Suresh, N. P. Rath, and S. Das, *J. Phys. Chem. C*, 2009, **113**, 11927–11935.
- 17 J. T. He, B. Xu, F. P. Chen, H. J. Xia, K. P. Li, L. Ye, W. J. Tian, *J. Phys. Chem. C*, 2009, **113**, 9892–9899.
- 18 Y. L. Wang, T. L. Liu, L. Y. Bu, J. F. Li, C. Yang, X. J. Li, Y. Tao, and W. J. Yang, *J. Phys. Chem. C*, 2012, **116**, 15576–15583.
- 19 F. Li, N. Gao, H. Xu, W. Liu, H. Shang, W. J. Yang, and M. Zhang, *Chem. Eur. J.*, 2014, **20**, 9991–9997.
- 20 L. Y. Bu, Y. P. Li, J. F. Wang, M. X. Sun, M. Zheng, W. Liu, S. F. Xue, and W. J. Yang, *Dyes and Pigments*, 2013, **99**, 833–838.
- 21 R. Thomas, S. Varghese, and G. U. Kulkarni, *J. Mater. Chem.*, 2009, **19**, 4401–4406.
- 22 Y. Fujiwara, R. Ozawa, D. Onuma, K. Suzuki, K. Yoza, and K. Kobayashi, *J. Org. Chem.*, 2013, **78**, 2206–2212.
- 23 Y. Sagara and T. Kato, *Nature Chemistry*, 2009, **1**, 605–610.
- 24 J. Kunzleman, M. Kinami, B. R. Crenshaw, J. D. Protasiewicz, C. Weder, *Adv Mater*, 2008, **20**, 119–122.
- 25 B. R. Crenshaw, C. Weder, *Chem Mater*, 2003, **15**, 4717–4724.
- 26 S. Y. Yoon, J. W. Chung, J. Gierschner, K. S. Kim, M. G. Choi, D. Kim, S. Y. Park, *J. Am. Chem. Soc.*, 2010, **132**, 13675–13683.
- 27 M. Martinez-Abadi, S. Varghese, R. Gimenez, and M. B. Ros, *J. Mater. Chem. C*, 2015, **3**, DOI: 10.1039/c5tc02852c.
- 28 N. D. Nguyen, G. Q. Zhang, J. W. Lu, A. E. Sherman, C. L. Fraser, *J. Mater. Chem.*, 2011, **21**, 8409–8415.
- 29 G. Q. Zhang, J. P. Singer, S. E. Kooi, R. E. Evans, E. L. Thomas, C. L. Fraser, *J. Mater. Chem.*, 2011, **21**, 8295–8299.
- 30 M. Sase, S. Yamaguchi, Y. Sagara, I. Yoshikawa, T. Mutai, K. Araki, *J. Mater. Chem.*, 2011, **21**, 8347–8354.
- 31 Y. Sagara, T. Mutai, I. Yoshikawa, K. Araki, *J. Am. Chem. Soc.*, 2007, **129**, 1520–1521.
- 32 C. Peebles, C. D. Wight, and B. L. Iverson, *J. Mater. Chem. C*, 2015, **3**, 12156–12163.
- 33 X. Zhang, Z. Chi, J. Zhang, H. Li, B. Xu, X. Li, S. Liu, Y. Zhang, and J. Xu, *J. Phys. Chem. B*, 2011, **115**, 7606–7611.
- 34 Y. Dong, B. Xu, J. Zhang, X. Tan, L. Wang, J. Chen, W. Tian, *Angew. Chem. Int. Ed.*, 2012, **51**, 10782–10785.
- 35 W. Liu, J. Wang, Y. Gao, Q. Sun, S. Xue, and W. Yang, *J. Mater. Chem. C*, 2014, **2**, 9028–9034.
- 36 P. Xue, B. Yao, X. Liu, J. Sun, P. Gong, Z. Zhang, C. Qian, Y. Zhang, and Ran Lu, *J. Mater. Chem. C*, 2015, **3**, 1018–1025.
- 37 Y. Liu, Y. Lei, F. Li, J. Chen, M. Liu, X. Huang, W. Gao, H. Wu, J. Ding, and Y. Cheng, *J. Mater. Chem. C*, 2015, **3**, DOI: 10.1039/c5tc02932e.
- 38 X. Zhang, Z. Chi, B. Xu, L. Jiang, X. Zhou, Y. Zhang, S. Liu, and J. Xu, *Chem. Commun.*, 2012, **48**, 10895–10897.
- 39 W. Liu, Y. Wang, L. Bu, J. Li, M. Sun, D. Zhang, M. Zheng, C. Yang, S. Xue, and W. Yang, *J. Lumin.*, 2013, **143**, 50–55.
- 40 M. Konishi, K. Fujita, and T. Tsutsui, *Mol. Cryst. Liq. Cryst.*, 2004, **425**, 11–19.
- 41 W. Liu, Y. Wang, M. Sun, D. Zhang, M. Zheng, and W. Yang, *Chem. Commun.*, 2012, **49**, 6042–6044.
- 42 M. Zheng, M. Sun, Y. Li, J. Wang, L. Bu, S. Xue, and W. Yang, *Dyes and Pigments*, 2014, **102**, 29–34.
- 43 Q. K. Sun, W. Liu, S. A. Ying, L. L. Wang, S. F. Xue, and W. J. Yang, *RSC Adv.*, 2015, **5**, 73046–73050.
- 44 Bu L, Sun M, Zhang D, Liu W, Wang Y, Zheng M, S. Xue, and W. J. Yang, *J. Mater. Chem. C*, 2013, **1**, 2028–2035.
- 45 M. Zheng, D. T. Zhang, M. X. Sun, Y. P. Li, T. L. Liu, S. F. Xue, and W. J. Yang, *J. Mater. Chem. C*, 2014, **2**, 1913–1920.

## Biographical notes:

Wenjun Yang received his BS, MS, and PhD degree in Polymer Chemistry and Physics from Jilin University, China. He carried out his postdoctoral work in National Tsinghua University (Taiwan of China) and research professor work in Korea University (South Korea) during 1998–2007. He is constantly on the faculty of Qingdao University of Science and Technology and promoted to Professor in 1995. His research was on the polymer synthesis and blend modification before 2000, and recent years is mainly on the synthetic chemistry and optoelectronic properties of novel anthracene- and arylidketo-based conjugated molecules.



Shanfeng Xue received his BS degree in Chemistry from Qufu Normal University (P. R. China) in 2007 and a PhD degree in Polymer Chemistry and Physics from Jilin University (P. R. China) in 2012. Now he works in Qingdao University of Science and Technology. His research interests include design, synthesis, structures, properties, and device performance of organic optoelectronic materials.

